Applied Materials Today xxx (xxxx) xxx

Contents lists available at ScienceDirect

Applied Materials Today

journal homepage: www.elsevier.com/locate/apmt

A disposable microfluidic-integrated hand-held plasmonic platform for protein detection

Fatih Inci[a,*,1], Yeşeren Saylan[a,b,1], Amideddin Mataji Kojouri[a], Mehmet Giray Ogut[a], Adil Denizli[b], Utkan Demirci[a,c,*]

[a] Bio-Acoustic MEMS in Medicine (BAMM) Laboratory, Canary Center at Stanford for Cancer Early Detection, Department of Radiology, Stanford School of Medicine, Stanford University, Palo Alto, CA, 94304, USA
[b] Department of Chemistry, Hacettepe University, Ankara, 06800, Turkey
[c] Department of Electrical Engineering (by courtesy), Stanford University, Stanford, CA, 94305, USA

ARTICLE INFO

Article history:
Received 8 July 2019
Received in revised form
18 September 2019
Accepted 28 September 2019

Keywords:
Point-of-care
Portable biosensors
Hemoglobin
Microfluidics
Plasmonic sensors

ABSTRACT

Healthcare is in the midst of a transformative shift from centralized care to point-of-care (POC). In this regard, recent efforts have focused on integration of biosensing technologies with clinical management and existing healthcare systems to improve the effectiveness and quality of care. Plasmonic technologies in particular, have been used for multiple applications in biosensing, pharmaceutical industry, food quality monitoring, and healthcare. However, bulky-sized platforms, expensive instrumentation, incomprehensive benchmarking, laborious protocols, and time-consuming processing steps remain challenges to adopt biosensing platforms to the POC settings. Here, we present a hand-held biosensing platform that integrates a plasmonic detection modality with a microfluidic chip. As a biological target model, we assess hemoglobin—an iron carrying protein in red blood cells. We comprehensively perform theoretical simulations and kinetic calculations to benchmark the platform performance. Overall, this miniaturized platform provides label-free detection, simple configuration for user-interface, facile sampling, assay-time down to 15–30 min, and inexpensive disposable chips. Therefore, this platform will potentially accelerate the deployment of portable biosensing systems for the POC and primary care settings.

1. Introduction

Contribution of biosensing technologies to current healthcare system is paramount [1–5]. As the world population is growing and aging, healthcare industry aims to replace existing biosensing tools with portable alternatives that can be practicable at doctors' offices and in-home care. Today the surge in computing power and technology have fashioned a foundation for portable biosensing platforms that can radically transform the effectiveness, mode, and quality of care and clinical research on a global scale [6]. Consequently, individuals can be potentially engaged with physicians at point-of-care (POC), primary care, and even at resource-constrained areas. Although this metamorphosis aims to minimize the need for sophisticated infrastructure, material cost and ease of operation are still remaining challenges.

As an example, hemoglobin is an iron-carrying protein in red blood cells and its concentration is closely correlated with several disorders and health condition such as thalassemia, cardiovascular diseases, anemia, sickle cell disease, leukemia, infectious diseases, and excessive loss of blood [7–9]. Monitoring hemoglobin concentrations in resource-limited settings is surrounded by expense, trained labor requirements, time and logistical constraints. For instance, gold standard method of malaria diagnosis is microscopy imaging of blood smear performed by a trained personnel, limiting its applicability to the POC settings [9,10]. Monitoring the elevated hemoglobin levels in serum is an alternative strategy for the diagnosis, however, the implementation of blood analyzers to the POC is still challenging. To add more examples, pathological conditions including ischemia reperfusion, sickle cell disease, and porphyria [11–13] are closely related with alterations in hemoglobin and heme (oxygen binding molecule on hemoglobin) levels in plasma. On the course of hemolytic processes, the elevated levels of heme and hemoglobin in plasma are in the range of 1–50 μM [10,14–16]. In the condition of sickle cell disease, this

* Corresponding authors at: Bio-Acoustic MEMS in Medicine (BAMM) Laboratory, Canary Center at Stanford for Cancer Early Detection, Department of Radiology, Stanford School of Medicine, Stanford University, Palo Alto, CA, 94304, USA.
E-mail addresses: finci@stanford.edu (F. Inci), utkan@stanford.edu (U. Demirci).
[1] These authors contributed equally.

https://doi.org/10.1016/j.apmt.2019.100478
2352-9407/

level is less than 20 μM, indicating that the elevated levels of cell-free plasma hemoglobin limits nitric oxide-mediated vasodilation in patients with sickle cell disease [17]. Diagnosis of these diseases therefore would greatly benefit from POC biosensing platforms with sensitive, inexpensive, rapid, easy-to-use, portable, and accurate fashions. In developed settings, testing and monitoring hemoglobin can be performed at centralized laboratories operated by trained personnel using expensive, automated, well-established, sensitive, quantitative assays such as spectrometric methods (*e.g.*, cyanide-based procedures, sodium lauryl sulphate technique, and azide-methemoglobin methods) [18]. However, these procedures are limited to clinical labs, and they are not suitable to fulfill the logistical and practical needs in terms of applications at the resource-limited settings. There are also some POC monitoring tools such as portable hemoglobinometers [19] and World Health Organization (WHO) hemoglobin color scale methods [20,21] for hemoglobin measurements. Despite the simplicity of operation of hemoglobinometers, they are prone to personnel errors and an intensive training is needed for the proper use [22,23]. Although the WHO hemoglobin color scale method is inexpensive and rapid, the diagnostic accuracy is very heterogeneous and less accurate as reported in the field studies [20,21]. To provide access to affordable, reliable, and easy-to-use POC monitoring without trading off the ability to perform clinically relevant assays, we [24–27] and others [28–31] have developed biosensing platforms on microfluidic chips, based on specific capture and sensing of biotargets. The POC platforms provide versatile, portable, and easy-to-use approaches with lower fabrication and assay expenses per sample, and remove the need for highly trained technicians to run the applications and to interpret results. These aspects overall allow these tools to be broadly available and easily applicable in resource-scarce environments [32].

Microfluidic technologies that require only a drop of specimen, offer significant advantages over traditional platforms *via* lab-chip approaches to detect biotargets from small volumes of biological specimens in a relatively short assay time [33]. These technologies can further improve the convenience of testing, hence potentially accelerating their access to the POC settings [6,34,35]. In addition, plasmonics, an emerging technology that exploits unique optical properties of metallic nanoparticles/nanostructures to enable manipulation of light at the nanoscale [36], has rapidly expanded our knowledge in biosensing field by denoting applications in pharmaceutical industry [37], clinical diagnostics [26,38], and environmental monitoring [39]. There have been proof-of-principle studies demonstrating that application of these Surface Plasmon Resonance (SPR) principles enabled development of tools for detection of various biotargets including cells, bacteria, antigens, antibodies, antibiotics, and nucleic acids [40–49]. Unlike traditional assays in biotarget detection (for example, immunoassays), which typically require one or more labels to amplify detection signal and lengthy labor-intensive sampling/washing steps, plasmonic-based biosensing devices detect biotargets in a label-free manner within a short assay time. In this regard, multiple plasmonic phenomena have been introduced through light coupling (*e.g.*, waveguide coupling, diffraction grating, Kretschmann and Otto configurations), localized plasmons, and nanoplasmonic array for a long time [26,50,51]. However, the fabrication of nanoplasmonic array requires expensive lithography methods, mask production, and nano-fabrication processes that are not suitable to create inexpensive sensors. Moreover, in localized plasmon strategies, handling nanoparticles and producing self-assembled plasmonic layers in a large-scale has been challenging due to variability of particle size and structures [52,53]. Among those strategies, light coupling for SPR strategy, especially Kretschmann configuration, has been utilized widely [54]. While the sensor fabrication requires plasmonic layer sputtering, it is relatively simple, reproducible, and also does not require any lithography steps and mask production. As the sensor is a disposable element for an assay, the fabrication strategy and cost are crucial for batch-fabrication and ease-of-translation to the clinic. Further, the SPR strategy has been miniaturized and integrated with smartphones to demonstrate the applicability of this phenomenon into portable systems without the need for bulky and benchtop systems [42,55]. However, from a POC perspective, some of these miniaturized systems integrate sophisticated thermal control and bulk refractive index compensation that increase the complexity of these platforms, which potentially limit the usability [56,57]. Although reference sensors and other instrumentations to account for the effects of nonspecific signals are significant units for these sensors [57,58], they potentially increase the costs of platform and assay, minimizing the applicability of such systems at the POC settings. Among those sensors, smartphone applications have been introduced to measure hemoglobin concentrations using either a 96-well format with a staining reagent or images from nails [59,60]. These platforms provide inexpensive measurements, however, they can only detect hemoglobin at mg/mL levels (6600 μg/mL [59] and <125,000 μg/mL [60]) and cannot provide a broad detection range (60,000 to 180,000 μg/mL [59] and 59,000 to 168,000 μg/mL [60]). Considering the clinical needs for the aforementioned diseases with hemolytic processes (1–50 μM or 64.1–3,305 μg/mL), their performances (detection limit and dynamic detection range) are limited to diagnose these conditions, and there is therefore a critical need for POC platforms with both affordable and sensitive features to measure hemoglobin levels in hemolytic and disease conditions.

To evaluate the utility and applicability of a platform before deploying into the POC settings, the WHO has provided framework criteria titled as "ASSURED" (affordable, sensitive, specific, user-friendly, rapid and robust, equipment-free and deliverable to end users) [61–63]. According to this criteria, true POC diagnostic tools do not require sophisticated laboratory infrastructure, expensive reagents/assay costs, and trained personnel to provide results. Further, a portable plasmonic-based technology has been reported for potential clinical applications, and we earlier demonstrated a proof-of-principle study focusing on the detection of bacteria through analyzing plasmonic responses in real-time [27]. Despite this specific body of proof-of-concept work, there has been minimal assessments of the portable biosensing platform and a comprehensive evaluation (*i.e.*, theoretical calculations of sensor performance and analytical kinetic models) of the platform for monitoring protein biotargets (*i.e.*, hemoglobin) binding. In general, the state of the art techniques are also lacking some of the key elements for a POC platform that are mentioned above [25]. Here, we present a major progress toward the extensive characterization of a portable biosensing platform for rapid, quantitative measurements of biotargets in real-time using a disposable microfluidic-plasmonic chip, which addresses some of the requirements at the POC settings. In essence, the presented tool already leverages inexpensive materials, easy-to-use chips, and comprehensive benchmarking (theoretical assessments and kinetic analysis), and thus, it can be further developed for user-friendly operation with the final goal of creating a robust, portable, and versatile biosensing platform for the POC settings. Briefly, the platform is a hand-held device that detects biotargets on a microfluidic chip, and a companion versatile surface chemistry that goes with these devices, specifically targeting hemoglobin as an exciting application in this case. The device is made out of affordable off-the-shelf plastics, double-sided adhesives, and a gold-coated substrate for a sensor. Introducing samples into the chip is facile and does not require any pre-training for personnel. The interface enables user-friendly operation and ease-of-readout within a short period of time (15–30 min).

To further validate the platform, we used hemoglobin molecules as a clinically relevant, biological target model. In this study, we

Please cite this article as: F. Inci, Y. Saylan, A.M. Kojouri et al., A disposable microfluidic-integrated hand-held plasmonic platform for protein detection, Appl. Mater. Today, https://doi.org/10.1016/j.apmt.2019.100478

Table 1
Comparison of the presented hand-held platform with the existing technologies for hemoglobin detection.

Parameters	Quartz crystal microbalance [94]	Hybrid organic-inorganic sensor [95]	SPR sensor [10]	Potentiometric sensor [96]	Smartphone application (App) [59,60]	This study
Sample load	Requires a pump	Requires a pump	Requires a pump	Not reported	Sampling to the 96-well plate [59] Taking images from nails [60]	Requires a pump
Detection conditions	10 mM PBS (pH 7.4) and 0.01 M HCl	50 mM Phosphate buffer (pH 7.4)	0.1 mM PBS (pH 7.4)	PBS (pH 7.0)	Images from blood samples after adding Hemocor-D reagent (staining) [59] Images from nails, no sampling [60]	PBS (pH 7.4)
Target	Hemoglobin	Hemoglobin	Apohemoglobin	Hemoglobin from bovine	Human hemoglobin [59,60]	Human hemoglobin
Detection range	0.2 to 1.0 μM	0.1 to 25 mg/mL	2.5 to 30.0 μM	0 to 250 μg/mL	60,000 to 180,000 μg/mL [59] 59,000 to 168,000 μg/mL [60]	5 μg/mL to 250 μg/mL
Limit of detection	0.15 μM	Not reported	2 μM	Not reported	6,600 μg/mL [59] <125,000 μg/mL [60]	Down to 5 μg/mL (0.078 μM)
Cost of assay	Not reported	Not reported	Not reported	Not reported	$0.15 excluding the cost of smartphone [59] Not reported	$4.18 per assay (chip cost)
User interface	Not reported	Not reported	Not reported	Not reported	Simple configuration for user-interface [59,60]	Simple configuration for user-interface
Theoretical simulations	Not reported	Not reported	Not reported	Not reported	Not reported	Plasmonic simulations Binding simulations
Kinetic analyses	Not reported	Not reported	Not reported	Not reported	Not reported	Equilibrium isotherm models (Scatchard, Langmuir, and Freundlich)
Advantages/disadvantages	Good sensitivity (down to 0.15 μM or 9.7 μg/mL) Requires precise temperature and oscillation controls Requires a pump	Moderate detection range (0.1 to 25 mg/mL or 1.55 μM to 387.6 μM) Requires GaAs-based molecular controllers Requires a pump	Moderate detection range (2.5 to 30.0 μM) A bulky, benchtop device Requires a pump	Good detection range (0 to 250 μg/mL or 0 to 3.876 μM) Requires ionic strength and ionic content control Requires a pump	User-friendly app Non-invasive measurement Portability Inexpensive assay High detection limits at mg/mL levels Low detection ranges (60,000 to 180,000 μg/mL and 59,000 to 168,000 μg/mL)	Good detection range (5 μg/mL to 250 μg/mL) Good detection limit (5 μg/mL or 0.078 μM) User-friendly interface Portability Inexpensive assay Conformation by theoretical and kinetic assessments Requires a pump

Please cite this article as: F. Inci, Y. Saylan, A.M. Kojouri et al., A disposable microfluidic-integrated hand-held plasmonic platform for protein detection, Appl. Mater. Today, https://doi.org/10.1016/j.apmt.2019.100478

benchmarked the performance of platform to detect hemoglobin molecules through theoretical assessments and kinetic analysis. We also evaluated the detection of hemoglobin in buffer and clinically relevant fluids, as well as assessed the specificity of sensor with solutions spiked with human serum albumin (HSA), making a compelling case to demonstrate that this platform would potentially create significant impact for the POC scenarios. In addition, we compared our platform with existing biosensing platforms (*i.e.*, quartz crystal microbalance, hybrid organic-inorganic sensor, potentiometric sensor, SPR sensor, miniaturized SPR, and smartphone-integrated SPR platform) that detect hemoglobin. In Table 1, we compared these platforms through theoretical assessment, analytical kinetic models, cost of assay, user-interface, sampling, and biosensing parameters (*e.g.*, detection range and limit of detection). Therefore, we have comprehensively evaluated the novel utility and applicability of the presented platform following the requirements for POC settings.

2. Results and discussion

2.1. Development of the portable platform and theoretical simulation

We designed our hand-held platform based on Kretschmann configuration, consisting (i) a 705 nm of LED with proper lens and polarizer for illuminating the surface, (ii) a glass prism, (iii) a CMOS sensor for measuring the amount of reflection from the surface, and (iv) a TV card for the connection between the platform and computer interface (Fig. 1a–b and Fig. S1, Supporting Information). In practice, at lower wavelengths in the visible range, gold does not show a good plasmonic response due to its complex permittivity [64]. However, working at higher wavelengths in near infrared (NIR) regime will potentially make the maintenance of the device complicated [65–67]. To create an easy-to-use and robust system, we hence integrated a 705-nm LED to benefit from both good plasmonic response in visible range with high performance keeping the maintenance of the device simple, which is important for reliable POC applications. The user-interface on our software provides real-time monitoring of resonance angle (R.A.) and reflectance spectrum at different angles (Fig. S2, Supporting Information). It consists of three layers: (i) a pyrex layer as base; (ii) a thin layer of titanium (5 nm) for the binding of gold to the pyrex; and (iii) a plasmonic gold layer (44 nm), where surface chemistry is applied for biotarget detection (Fig. 1c).

To evaluate performance of the platform, we first performed calculations based on a transfer matrix formalism in which the parameters of the analytical model were estimated based on the measured spectra (Supporting Information). According to our calculations, the surface plasmons are excited at an angle of 69.2° (Fig. 1c–d). The simulations show that if a typical protein layer with a thickness of 5 nm (n = 1.45) [68] covers the surface of plasmonic sensor, its R.A. will shift about 0.56 degrees (Fig. 1d), which is mainly due to the high field enhancement near the metal-solution interface (Fig. 1d, inset).

To capture biotargets on the plasmonic chip, we also designed a specific surface chemistry approach for hemoglobin detection as a model biological molecule. The surface of plasmonic chip was decorated with three layers: (i) chemical layer including 11-mercaptoundecanoicacid (MUA) and N-(3-dimethylaminopropyl)-N′-ethyl carbodiimide hydrochloride (EDC)/N-hydroxy succinimide (NHS) coupling to form succinimide groups; (ii) protein G layer as an antibody anchor; and (iii) antibody layer for detection (Fig. 1e).

Table 2
The parameters of plasmonic surface and adsorbed protein layers.

Layer	Refractive index	Thickness (nm)	References
Glass (NBK7)	1.5129	–	[97]
Titanium	2.4274 - 3.1605j	5.2	[64]
Gold	0.1616 - 4.02j	44.1	[64]
Chemical Layer	1.4	1.71	[98]
Protein G	1.54	1.35	[99]
Antibody	1.36	7	[99]
PBS Solution	1.3324	–	[100]

2.2. Evaluating surface modification and correlating experimental data with theoretical simulations

Each surface chemistry layer and washing step were applied on the plasmonic chip, and the R.A. alterations were monitored in real-time (Fig. 2a). To characterize binding events, we recorded angular interrogation measurements at each step of surface chemistry, and then, estimated the refractive index of the adsorbed layers-based on our theoretical calculations (Fig. 2b–d, Supporting Information). The extracted values for the parameters of the plasmonic sensor and the adsorbed protein layers were summarized in Table 2 and Tables S1–S2 (Supporting Information). To examine the reflection spectra on both theoretical and experimental data, we calculated R.A. and the width of R.A. ($\Delta\theta$) for chemical layer, protein G, and antibody layers (Fig. 2e) [69]. In experimental results, we observed the R.A. values at 69.29°, 69.50°, and 69.68° for chemical layer, protein G, and antibody, respectively. Theoretical calculations demonstrated resonances occur at angle of 69.24°, 69.48°, and 69.66° for the same layers. For the $\Delta\theta$, theoretical calculations indicated a width of 2.21°, 2.25°, and 2.15° for chemical layer, protein G, and antibody, respectively. The experiments resulted in 2.20°, 2.38°, and 2.48° for those layers. In Fig. 2e, we observed that adsorption of proteins resulted in an increase of resonance width. Comparing the theoretical and experimental results, the $\Delta\theta$ values are almost same before addition of protein and antibody layers. When a protein or antibody layer is bound to the surface, the resonance is usually widened, which can be potentially related to the optical absorption and scattering by the protein or antibody layers [64]. The mostly employed model in the literature for describing the binding events on plasmonic surfaces assumes the layer as a thin loss-less uniform dielectric layer, which neglects possible absorption of light by proteins and its scattering due to non-uniformity of the covered surface [65–67].

To confirm surface functionalization, we performed Fourier Transform Infrared-Attenuated Total Reflectance (FTIR-ATR) measurements on the modified gold surfaces (Fig. 2f). As the surface chemistry approach contains protein G and antibody, we focused on the fingerprint regions of peptide bonds from 1400 cm^{-1} to 3000 cm^{-1}. The intensity band appearing in the region of 2929 cm^{-1} was assigned to C–H stretching vibrations. The amide I band at ~1700 cm^{-1} occurred at the C=O stretching vibrations. The amide II band at the region 1475 cm^{-1} was observed for N–H stretching vibrations. At these wavelength locations, we did not observe any significant peaks on the bare (unmodified) gold surface. Both bare and modified surfaces provided two peaks at ~2000 cm^{-1}, which might be caused by pyrex material and metal layer. We then characterized hydrophilicity properties of the bare (Fig. 2f-inset 1) and modified gold surfaces (Fig. 2f-inset 2). The contact angle value of bare gold surfaces decreased from 83.5° ± 3.5 to 61.1° ± 3.4 indicating that we achieved the layer-by-layer surface modification and created a more hydrophilic surface (Figs. S3–S4, Supporting Information). Cumulatively, these two different characterization methods confirmed that our protein-based surface modification was successfully applied to the chip surfaces.

Please cite this article as: F. Inci, Y. Saylan, A.M. Kojouri et al., A disposable microfluidic-integrated hand-held plasmonic platform for protein detection, Appl. Mater. Today, https://doi.org/10.1016/j.apmt.2019.100478

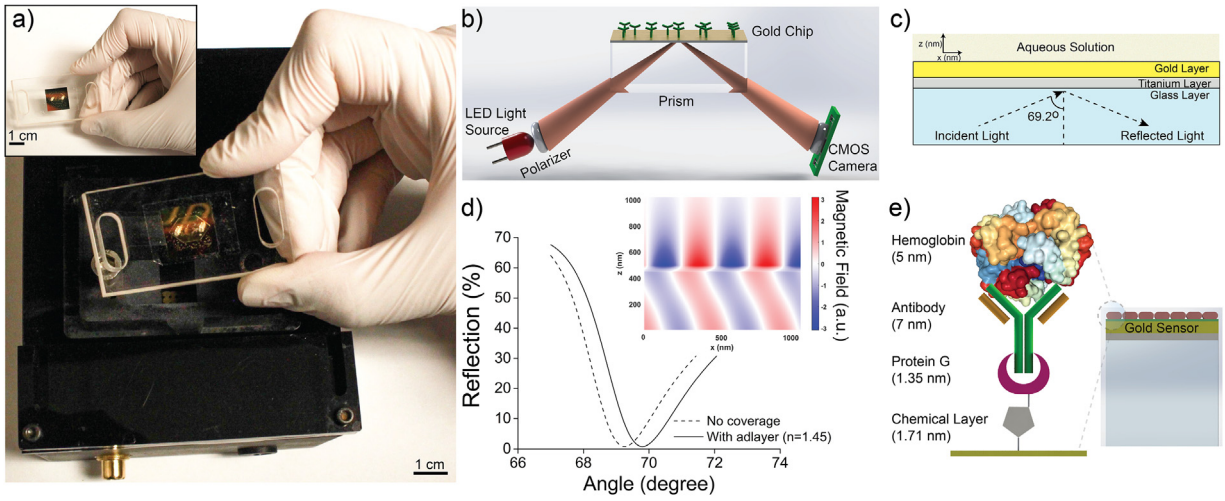

Fig. 1. Hand-held plasmonic platform. (a) A hand-held plasmonic device and a microfluidic-integrated plasmonic chip are presented. The chip consists of two layers of PMMA and a gold-coated chip, which are assembled with double-sided adhesive (DSA) tapes. Samples are introduced through the inlet port and waste is collected from the outlet port. (b) The platform consists of a light emitting diode (LED) to illuminate a cylindrical lens, which focuses the light onto a rectangular prism. The reflected light is captured on a CMOS sensor, and the captured image is transferred to a computer via the control circuitry and a TV card. (c) Gold-coated chips are fabricated on a glass (pyrex) wafer by depositing 5 nm of titanium layer and 44 nm of gold layer, respectively. (d) The binding of a homogenous adlayer ($n_{adlayer}$ = 1.45) with 5 nm of thickness generates a change in resonance angle of the gold chip. Magnetic field distribution around the plasmonic surface is visualized when the surface is illuminated by a plane-wave from the bottom. (e) The chip surface is activated with three layers: (i) chemical layer with succinimide ending; (ii) protein G layer; and (iii) antibody layer to capture hemoglobin molecules (Protein Data Bank: 2HCO). Scale bars represent 1 cm.

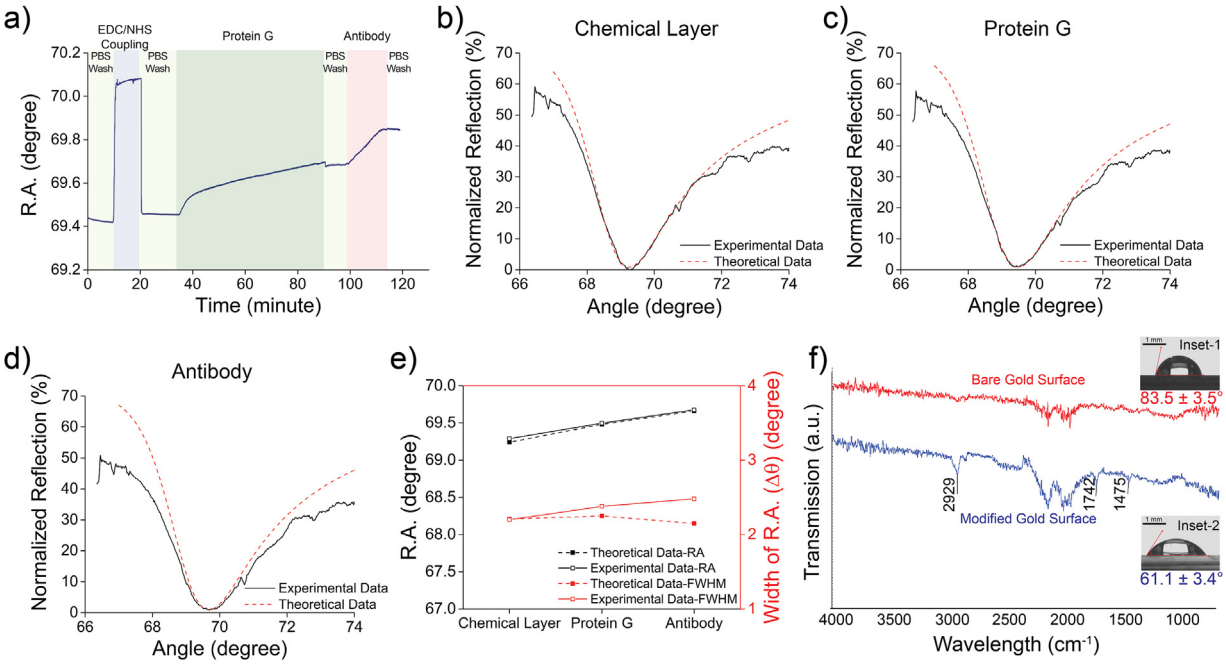

Fig. 2. Theoretical and experimental evaluations of surface chemistry. (a) Surface modifications on the plasmonic chip are monitored in real-time, and the data is presented as a resonance angle (R.A.). Experimental (solid line) and theoretical (dashed line) data are demonstrated in the plots. Reflection spectra are measured and calculated (b) when only chemical layer is present; (c) when both chemical layer and protein G layer are present; and (d) when all three layers including antibody layer are present on the chip surface. (e) R.A. and the width of R.A. ($\Delta\theta$) values are calculated for both experimental and theoretical assessments using the corresponding reflection spectra according to the curve of reflection spectrum. (f) Surface modifications are confirmed by Fourier-Transform Infrared (FTIR)-Attenuated Total Reflectance (ATR) Spectroscopy and contact angle measurements in terms of spectra values, chemical bonds and hydrophilicity properties. The intensity band appearing in the region of 2929 cm^{-1} is assigned to C–H stretching vibrations. The amide I band at ~1700 cm^{-1} exhibits at the C=O stretching vibrations. The amide II band is located at the region 1475 cm^{-1} that has been designated to N–H stretching vibrations. In the contact angle measurements, the modified surfaces result in more hydrophilic characteristics (inset-2) compared to the bare surfaces (inset-1). Scale bars represent 1 mm.

2.3. Evaluating protein detection on the hand-held platform

To assess the binding performance of platform, we applied multiple hemoglobin concentrations, ranging from 5 to 250 μg/mL and the results were monitored as R.A. shifts (Fig. 3a and Fig. S5, Supporting Information). Briefly, after surface chemistry was decorated on the sensor surface, (i) a baseline was created with PBS flow at 5 μL/min using a syringe pump; (ii) hemoglobin solution at the defined concentration was then applied to the surface; and (iii) a second PBS flow was used to remove unbound hemoglobin molecules from the surface. Hemoglobin solutions resulted in an observable R.A. shift value at the resonance peak angle, ranging

Please cite this article as: F. Inci, Y. Saylan, A.M. Kojouri et al., A disposable microfluidic-integrated hand-held plasmonic platform for protein detection, Appl. Mater. Today, https://doi.org/10.1016/j.apmt.2019.100478

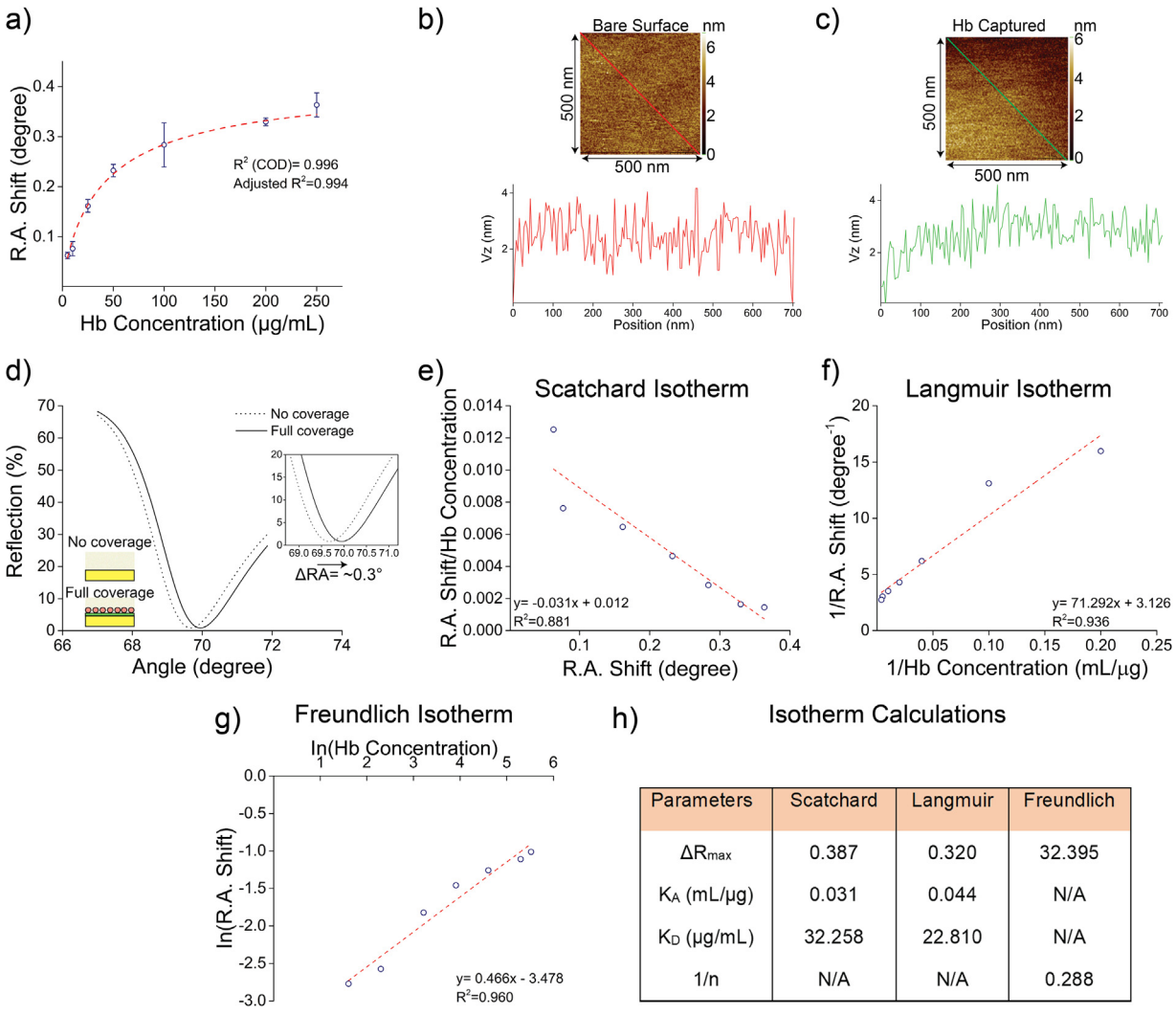

Parameters	Scatchard	Langmuir	Freundlich
ΔR_{max}	0.387	0.320	32.395
K_A (mL/µg)	0.031	0.044	N/A
K_D (µg/mL)	32.258	22.810	N/A
1/n	N/A	N/A	0.288

Fig. 3. Hemoglobin detection on plasmonic chips. (a) Various concentrations of hemoglobin, ranging from 5 µg/mL to 250 µg/mL are introduced to the gold chips, and the changes in resonance angle (R.A.) are plotted across different hemoglobin concentrations (n = 3–4). (b–c) Atomic Force Microscopy (AFM) is utilized to evaluate roughness changes on the bare (non-modified) and modified (hemoglobin captured sensor) gold surfaces. (d) Theoretical assessments are applied to examine the changes in R.A. when the chip is (i) not covered and (ii) fully covered with hemoglobin molecules. (e) Scatchard adsorption isotherm allows to evaluate the experimental data for reversible host-guest interactions and identifies total binding sites when the host is at the equilibrium condition. (f) Langmuir adsorption isotherm is a homogeneous binding model whereas (g) Freundlich isotherm demonstrates a heterogeneous binding on the surface. (h) Isotherm calculations are presented in the table.

from 0.063° ± 0.006 to 0.363° ± 0.024 for the concentrations of 5–250 µg/mL. We observed a 0.996 of correlation coefficient in the standard curve. Comparing to inexpensive alternatives such as smartphone-based platforms, our platform provides a wider detection range from 5 µg/mL to 250 µg/mL within the clinical ranges of hemolytic process and sickle cell disease, and can detect hemoglobin down to 5 µg/mL (0.078 µM) (Table 1).

We performed Atomic Force Microscopy (AFM) experiments to evaluate the roughness of the bare and modified surfaces (after hemoglobin capture) (Fig. 3b–c). By examining the height variations along the hypotenuse of each scanned image (0.5 µm × 0.5 µm) [70–72], we found out that the bare surface was more rough compared to the surface after hemoglobin capture.

2.4. Examining theoretical simulation for surface coverage

We have performed theoretical assessments to understand the R.A. alterations while hemoglobin captured on the chip surface (Fig. 3d). When no hemoglobin (no coverage: the sensor surface is modified up to antibody layer) is captured by the antibodies, the R.A. is 69.66°. By decorating the entire surface with hemoglobin modelled as a homogenous layer with thickness of 5 nm and refractive index of 1.39 (Supplementary Information), there will be a shift of ~0.3° (Fig. 3d). Partially coverage of the surface with hemoglobin can be modelled by a homogenous layer with the same height but with lower refractive index (Supplementary Information). This reduction in refractive index will result in a smaller shift in the R.A., which is also observed in our concentration-based R.A. plot. In the experiments, hemoglobin concentrations from 100 to 250 µg/mL resulted in R.A. shifts between 0.284° ± 0.044 and 0.363° ± 0.024 (Fig. 3a). Considering both theoretical calculations and experimental data, there might be an excessive amount of hemoglobin on the surface after ~0.3° of R.A. shift since the surface is fully covered on that R.A. value.

2.5. Evaluating equilibrium isotherm models for hemoglobin binding on-chip

To determine the interactions between hemoglobin molecules and antibody-coated gold chips, we applied three different equilibrium isotherm models, *i.e.*, Scatchard, Langmuir, and Freundlich (Fig. 3e–g) (Supporting Information) [73–78]. This analysis enabled

Please cite this article as: F. Inci, Y. Saylan, A.M. Kojouri et al., A disposable microfluidic-integrated hand-held plasmonic platform for protein detection, Appl. Mater. Today, https://doi.org/10.1016/j.apmt.2019.100478

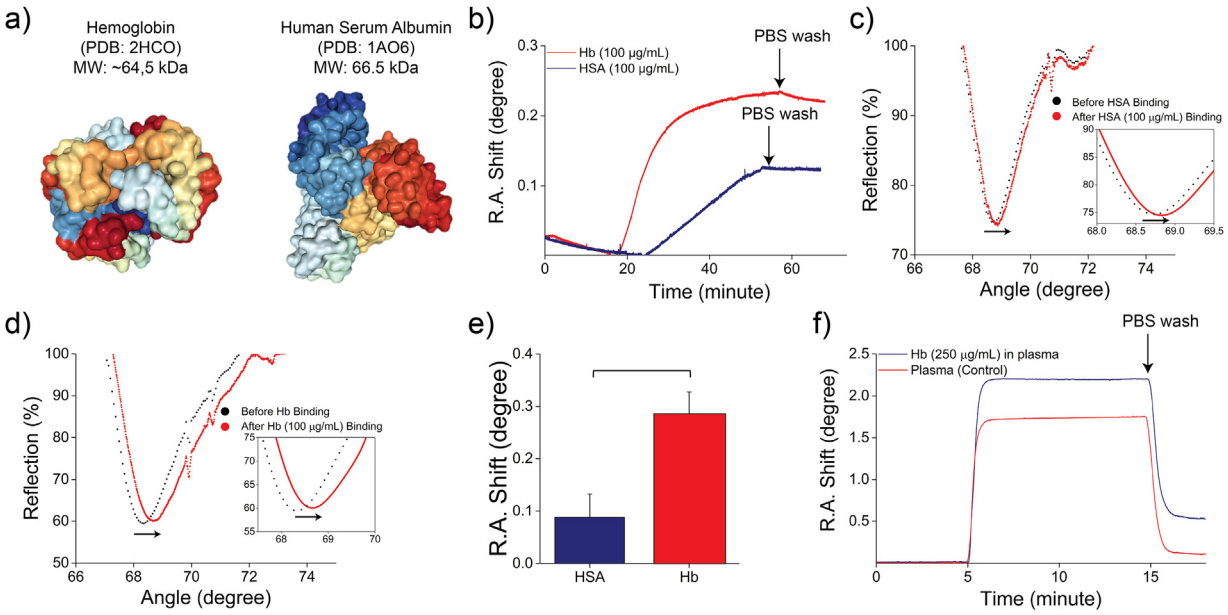

Fig. 4. Evaluation of specificity and testing the platform with clinically relevant media. (a) Molecular structures of hemoglobin (Hb) and human serum albumin (HSA) are obtained from Protein Data Bank (2HCO and 1AO6). (b–d) In the experiments, the chip surfaces are decorated with anti-human Hb antibodies, and either hemoglobin or HSA is applied to chip surfaces. Real-time analysis denotes the capture/binding events of these proteins. Changes in resonance angle (R.A.) were plotted before and after capture/binding events of Hb and HSA. Polynomial curve fitting was applied to the plots in the insets. (e) As a result, Hb binding provided statistically significant R.A. change compared to the binding of HSA ($n = 3$, $p < 0.05$). For statistical analysis, we used Student's *t*-test with the statistical significance threshold set at 0.05 ($p < 0.05$). Horizontal bracket demonstrates statistically significant differences between groups. Data is represented with average value ± standard deviation ($n = 3$). (f) The chip surface is coated with anti-human hemoglobin antibodies, and either hemoglobin spiked in plasma or only plasma sample (control) is applied to chip surfaces. The R.A. changes are monitored in real-time.

us to evaluate the sensor performance and also characterize the host-guest interactions with established binding kinetics.

In the analysis, all isotherm models (except Scatchard) provided high correlation coefficient values (>0.93). Although the Scatchard model pointed out surface heterogeneity due to its lower correlation coefficient value (0.881), the adsorption isotherms could be well expressed by the Langmuir model, which resulted in higher correlation coefficient ($R^2 = 0.936$) compared to the Scatchard model, indicating the formation of monolayer binding on the gold sensor. Surface heterogeneity observed on the curve of Scatchard model can be explained through multiple binding locations, which have similar affinity for hemoglobin binding [79]. Even though the correlation coefficients of Freundlich ($R^2 = 0.960$) and Langmuir models ($R^2 = 0.936$) were more than 0.93, the ΔRA_{max} value of Langmuir model ($\Delta RA_{max} = 0.320$) agreed with the experimental data ($\Delta RA_{max} = 0.363$) compared to the Freundlich model ($\Delta RA_{max} = 32.395$). Overall, Fig. 3h demonstrated clearly that the Langmuir isotherm model more accurately described hemoglobin binding on the gold sensor, likely due to the homogenous binding locations formed on the surface [73]. Considering theoretical calculations (Fig. 3d) and kinetic isotherm models (Fig. 3e–g), the majority of hemoglobin binding generated a monolayer structure and there might be heterogeneous structures on the surface due to the result of Scatchard model. According to the Langmuir isotherm model, the kinetic parameters (K_A and K_D) of hemoglobin binding were calculated as 0.044 and 22.810, respectively (Fig. 3h).

2.6. Evaluating specificity

Specificity refers to the ability of an assay to measure on particular substance rather than others in a sample [80]. Here, as a specificity model, we chose human serum albumin (HSA), which is the most abundant protein in human blood and it has very close molecular weight with hemoglobin (Fig. 4a) [81]. In the experimental sets, we decorated the chip surfaces with anti-human hemoglobin antibodies, and applied either hemoglobin or HSA to chip surfaces. As a result, we observed R.A. shifts and the signal was then stabilized after the washing step at both sets (Fig. 4b–d). According to the statistical assessments, the binding of hemoglobin provided significantly higher R.A. shifts (~3 times higher) compared to the HSA binding ($n = 3$, $p < 0.05$) (Fig. 4e). This indicated that the surface chemistry approach and antibody provided specific binding of hemoglobin to the surface.

In addition, non-specific binding is one of the caveats that biosensor platforms face, and it could potentially occur at multiple regions of sensor, including functionalized, passivated, and untreated areas [26]. To minimize the non-specific bindings, the chip surface could be modified with anti-fouling agents such as proteins (*e.g.*, bovine serum albumin, casein, glycine, and gelatin), chemical linkers (*e.g.*, thiol-linkers), and polymeric compounds (*e.g.*, PEG linkers) as we and others demonstrated earlier [25,82–87]. Therefore, the signal change and background could be managed to minimize any potential non-specific bindings. By integrating one of anti-fouling agents listed here, specificity and sensitivity performance of the current chip would be potentially increased.

2.7. Testing with clinically relevant matrix

To create a compelling case and evaluate the chip performance for POC scenarios, we chose human plasma as a clinically relevant media (Fig. 4f). In the experimental sets, we decorated the chip surfaces with anti-human hemoglobin antibodies and applied either hemoglobin (250 µg/mL)-spiked in plasma or plasma (control) to chip surfaces. As the plasma has highly dense structure with high refractive index value, the R.A. resulted in a high change. After the signal stabilized, we performed a PBS wash step and observed that the R.A. levels decreased in both experimental sets. Briefly, in the control set, we observed that some of the plasma proteins bound to the chip surface non-specifically, which resulted in a

Please cite this article as: F. Inci, Y. Saylan, A.M. Kojouri et al., A disposable microfluidic-integrated hand-held plasmonic platform for protein detection, Appl. Mater. Today, https://doi.org/10.1016/j.apmt.2019.100478

shift of ∼0.143° as close as the binding of HSA experiments. The hemoglobin-spiked in plasma set resulted in higher R.A. changes compared to the control set. As plasma proteins non-specifically bound to the chip surface, the R.A. value (∼0.5°) was higher than that of hemoglobin in PBS experiment (∼0.363°), indicating that the R.A. change was a combination of signals from the binding of hemoglobin and plasma proteins. In addition, the clinical cut-off for hemoglobin is 50 μg/mL in serum. The microfluidic chip also allows us to introduce samples serially, and hence, accumulates more captured target moieties on the surface by multiplying the ∼50–150 μL of used sample volume to 300 μL and allowing us to reduce the sensing down to the clinical cut-off.

Clinically relevant media (*e.g.*, plasma, blood, tears, urine, and saliva) hold multiple intrinsic structures including contents, pH, and ionic strength [25]. Especially, blood and plasma samples contain multiple proteins and lipids that significantly interfere with sensor performance such as sensitivity and specificity. In particular, SPR-type modalities, as label-free methods, are much less specific for detecting protein targets from complex specimens for quantitative biomarker measurement in clinical specimens. In this regard, non-specific binding to the chip surface is one of the major bottlenecks for binding and detection experiments as the concentration of other compounds is relatively higher than the target concentration [88,89]. As aforementioned, integrating anti-fouling agents with the surface chemistry approach would potentially increase sensitivity and specificity performance of the sensors when detecting biotargets in clinically relevant matrices [25,82–87]. Therefore, the current system could be adapted to the detection of various biological and chemical targets in the other clinical matrices and patient samples in the future.

3. Conclusion

Standard hemoglobin assays in routine clinical practice take place in a centralized laboratory and involve blood collection by venipuncture, plasma separation by centrifuge, and assaying the specimen employing a commercial platform. These methods are demanding in cost, time, and they require well-trained personnel and regular maintenance. These requirements are not fit for processing assays in resource-scarce settings. The developed platform that we present here shows an inexpensive assay as an alternative to automated instruments used in centralized laboratories. Additionally, our platform presents some technical and practical advantages over other platforms developed with SPR-based microfluidic tools. The chamber-flow design of our platform allows it to sequentially process a fingerprick volume of plasma by moving the target fluid specimens over a functionalized surface, which allows the device to be disposable, single-time use, portable, and compact. From a clinical diagnostic perspective, disposability is one of the crucial points that help eliminating potential contaminations from sample-to-sample and patient-to-patient. In this regard, the chip will be decorated with the surface chemistry, and it will be disposable and single-time use for diagnosis purposes. Further, the surface chemistry on the chip has a versatile characteristic, and sampling/sensing procedure can be easily modified with desorption agents to reuse the chip multiple times for research purposes as reported in the literature [78,90,91]. However, adding desorption agents to the current procedure will increase the number of steps and manipulations needed by the end-user. Considering potential contaminations and user-friendly approach, we designed the current chip with disposable fashion.

Since this platform uses pre-fabricated chips containing specific chemistry on a plasmonic sensor, the end-user will only have to load a sample into the platform to monitor the results within 15–30 min at ambient temperature. With the current design and configuration, no complicated operations are performed by the end-user. The device can also be compartmentalized into multiple separate lanes of plasma and controls, which can test multiple independent assays in parallel. The platform does not require any pre-processing of samples or introduction of additional reagents into the microfluidic device after the clinical specimen is loaded on chip using a single-rate flow. The specimen can be potentially collected by a capillary from a fingerprick. All these steps can be performed on a POC setting and the entire procedure does not require skilled personnel. This tool is currently designed within lab settings and further commercial development can be brought in the next stage to turn the platform into a single push of a button taking it beyond academic settings. Additionally, since the data analysis is not computationally intense, the data acquisition and analysis can be easily performed on a smartphone to reduce the total footprint and accelerate to access testing in remote settings. Therefore, we can potentially reduce the cost of assay.

The platform is versatile with easily modifiable microfluidic designs and by changing the surface chemistry (the last step being modifiable by changing the final attached antibody), the platform can be applied to detect multiple biomarkers. To evaluate the performance of platform, we employed detection of hemoglobin molecules as a model biotarget using anti-human hemoglobin antibodies. As demonstrated, the platform can detect hemoglobin specifically in contrast to HSA molecules due to the specificity of antibody. As the surface chemistry is designed to immobilize antibodies to the chip surface, by only changing the antibody type, we can further broaden the applications of this versatile platform towards other target molecules. This unique capability is introduced by moving the targets on the specifically functionalized substrate through the channel for the specific binding step of the assay followed by the plasmonic sensing of bound targets. In addition, other recognition elements, such as carbohydrates, nucleic acids, peptides, and aptamers, could be easily integrated to the platform through various surface chemistry approaches, such as chemical binding, biotin-avidin interactions, and thiolization [26,50,92].

Further, we addressed multiple engineering challenges in design, fabrication, and benchmarking aspects, including: we (i) designed the chip to match the biosensor optics; (ii) integrated a gold-coated bottom sensor layer with a top channel to allow microfluidic integration; (iii) fabricated this chip to match biosensor optics; (iv) made this chip perform the same way from sample-to-sample and batch-to-batch of fabrication; (v) evaluated the chip shelf-life due to any adverse effects such as oxidization; (vi) performed surface chemistry on biosensor surface of the chip without perturbing microfluidic device integrity; (vii) optimized fabrication process steps in order to avoid any leakages during the testing of plasma which in return would damage the optical sensors; (viii) designed a top cover to perform data collection under ambient conditions without jeopardizing platform mobility or increasing weight of size; (ix) through this top cover introduced microfluidic tubings in and out of the integrated device; (x) ensured a design, where the chip is disposable and inexpensive without changing any components on the biosensing reader component. This is critical given the chip cost $4.18 and the reader can cost up to $114.25. (xi) In this microfluidic integrated biosensor, surfaces are not openly accessible as they sit inside a channel. Hence, surface chemistry was performed through only inlet and outlet ports. Under these circumstances, we developed a reliable and repeatable surface chemistry for device performance. (xii) We used the biosensor as a confirmatory tool in real-time to evaluate and monitor the multi-layer surface chemistry as it is built on the chip through fluid flowing into the channels to overcome the described inaccessibility to the functionalized device surfaces. (xiii) We disengaged microfluidic chip and the reader to ensure

Please cite this article as: F. Inci, Y. Saylan, A.M. Kojouri et al., A disposable microfluidic-integrated hand-held plasmonic platform for protein detection, Appl. Mater. Today, https://doi.org/10.1016/j.apmt.2019.100478

that the biological matrix such as plasma get collected in a closed reservoir without contaminating sensor optics of the reader. (xiv) We addressed challenges around plasma versus PBS. We realized that the surface chemistry was not enough when we perform the experiments on the PBS, we had to further optimize the surface chemistry for other complex matrices. (xv) We further analyzed kinetic parameters and isotherm models of hemoglobin binding to the surface, and comprehensively evaluated the experimental data for each surface chemistry step with theoretical simulations. (xvi) We also developed a simple user-interface to monitor and acquire data in real-time.

Moreover, this platform can be further improved by introducing new design aspects. First, the current design of chips has one microchannel and process ~50–150 μL of sample volume, which is typical in a biological test. By integrating multiple channels and different channel designs, the platform can potentially handle more than one sample per chip, and it can be versatile to the detection of multiple targets on the same chip. Second, our system currently utilizes a microfluidic pump that is operated a single flow rate, which can be automated into any integrated system that would keep the whole system still portable and battery operated, thereby potentially further minimizing personnel integration. Third, we decorated the microchannels with anti-human hemoglobin antibodies in the current study. Although cold transport and storage for microchips with surface chemistry and antibodies is crucial, we have presented multiple strategies, *i.e.*, dry-storage of microchips, prolonging their stability and shelf life up to 6 months at the POC settings [93]. For the dried surfaces, reactivation of surface chemistry and antibodies on-chip requires only introducing of PBS in less than a minute before use, which will not significantly change our current procedure for detection. Fourth, the current microfluidic chip utilizes affordable materials and one chip costs $4.18, including two layers of poly methyl methacrylate (PMMA), two layers of double-sided adhesive (DSA), one gold sensor, chemical agents, protein G, and antibody (Fig. S6, Supporting Information). The chip cost we report here is based on what we experience building it manually at a lab setting. The gold sensor comprises the majority of total cost, and it can be potentially reduced with large-scale production such as using the injection molding strategy that tends to potentially reduce the cost to pennies. In addition, a hand-held platform is designed on a power distribution circuit board, which costs $114.25 (without boxing) (Fig. S7, Supporting Information). Large-scale production or purchase of chemicals, proteins, antibodies, and circuit elements (especially TV card and CMOS) will significantly reduce the cost of the entire platform. Fifth, we evaluated the batch-to-batch and inter-operator variations with >35 chips, and the chips provided reliable and repeatable results when operated by four different people in the lab setting. A larger sample and user study would be necessary for more conclusive and quantitative results around batch-to-batch and user-to-user variability.

Overall, hemoglobin-associated diseases are major adverse events, where simple systems can have a positive clinical impact. The presented hand-held platform addresses critical technical and logistic challenges, potentially accelerating the integration of portable biosensing systems into the POC settings. In addition, the ability of our platform (i) to provide results in a short assay time, (ii) utilize inexpensive materials for disposable microfluidic device, and (iii) require minimum user involvement and facile sampling can create new avenues in diagnosing patients at the POC and primary care settings. In the future, we anticipate that the presented platform will ultimately represent a laboratory-quality platform, integrating advantages of microfluidic and micro-scale technologies to build a disposable chip and a user-friendly portable plasmonic reader platform simplifying and diminishing the assay cost for diagnosis and prognosis of vascular and blood-based diseases. Conceivably, further development for such a versatile platform combined with automation would facilitate creation of other clinically relevant POC assays and applications going after multiple markers and biotargets in various plausible settings at home, primary care, hospital bedside, and at resource-limited settings. Here, we showed what this technology can achieve as a proof-of-concept testing the tool's limitations without seeking any commercialization considerations. Through commercial development process, the presented system could be fully automated in a company setting and commercialized to be applicable for disease diagnostics at the clinic, especially at the POC settings.

4. Experimental

4.1. Materials

11-mercaptoundecanoicacid (MUA, 450561), N-(3-dimethylaminopropyl)-N′-ethyl carbodiimide hydrochloride (EDC, 03450), MES (M3671), N-hydroxy succinimide (NHS, 130672), ammonium hydroxide (221228), and hydrogen peroxide solution (H1009) were purchased from Sigma Aldrich. Protein G (21193), 2-propanol (AA36644K7), and human hemoglobin antibody (MA5-14708) were obtained from Thermo Scientific. Human hemoglobin (MBS173108) was purchased from MyBioSource. Ethanol (200 proofs) were obtained from Goldshield (412811). For the microfluidic chip fabrication, poly methyl methacrylate (PMMA, McMaster Carr, Atlanta, GA) and double-sided adhesive (DSA, iTapestore, Scotch Plains, NJ) were used.

4.2. Gold sensor fabrication

Glass wafers (Pyrex, double side polished wafers with diameter 100 mm of diameter and 475–575 μm of thickness) were purchased from WRS Materials, and were cleaned with piranha solution. The wafers were then placed on a spin-coater (Lesker), and the system was operated at 200 W (DC), 3 mT of pressure under Ar 50 sccm. The wafers were coated with 5 nm of titanium, followed by a 44 nm of gold on the same side through 0.83 A/s and 0.8 A/s of deposition rates, respectively. Later, the metal coated wafers were spin-coated with a 1 μm layer of photoresist (Shipley 3612) at 5.5k/rpm for 40 s, followed by a baking step at 90 °C for 1 min. The wafers were diced in 1.4 cm × 1.4 cm chips using a mechanical dicer (DISCO DAD3240).

4.3. Microfluidic chip fabrication

The microfluidic chips had three main components: (i) two poly(methyl methacrylate) (PMMA) layers (3.2 mm of thickness for each layer), (ii) two double-sided adhesive (DSA) films (50 μm of thickness for each layer), and (iii) a gold sensor (1.4 mm × 1.4 mm). In this design, the larger DSA film (57 mm × 30.9 mm) enabled to assemble two PMMA layers and the smaller DSA film (5.5 mm × 18.5 mm) was used to integrate the gold sensor and provide microfluidic channels. Versa LASER (Universal Laser Systems Inc., Scottsdale, AZ) was used to design and cut PMMA layers and DSA films. Inlets and outlets (0.65 mm in diameter) of the microfluidic chips were cut on two PMMA layers. The microfluidic chips were then mounted by assembling these three components. Gold sensors were used as a base material, where we performed surface chemistry for hemoglobin detection.

4.4. Cleaning of gold sensors

Before assembling microfluidic chips, we cleaned the gold sensor surfaces with solvents to remove impurities. Briefly, the sensors were submerged in an isopropanol:ethanol (1:1) bath and heated 60 °C for 5 min. The sensors were then washed with deionized water and dried with the filtered compressed air. Followed by the

Please cite this article as: F. Inci, Y. Saylan, A.M. Kojouri et al., A disposable microfluidic-integrated hand-held plasmonic platform for protein detection, Appl. Mater. Today, https://doi.org/10.1016/j.apmt.2019.100478

first step of cleaning, the sensors were submerged in a piranha solution (H_2O:H_2O_2:NH_4OH, 5:1:1) for 5 min. They were then rinsed with ethanol and drying with the filtered compressed air in order to assemble with microfluidic chip.

4.5. Surface chemistry

After the cleaning step, the gold sensors were modified with a layer-by-layer surface chemistry approach. Briefly, the gold surfaces were incubated with MUA (10 mM in ethanol) overnight at room temperature, therefore carboxyl groups were originated onto the surface. The sensor was then assembled with the microfluidic chip, and the tubings were attached to the inlet and outlet ports using epoxy. N-(3-dimethylaminopropyl)-N′-ethyl carbodiimide hydrochloride (EDC, 100 mM)/N-hydroxy succinimide (NHS, 50 mM) mixture (100 μL) was then introduced into the microchannel via either a syringe pump or manually and incubated for 30 min at room temperature. EDC and NHS solutions were prepared in 50 mM of MES buffer (pH 5.0). Basically, EDC reacts with carboxyl groups to form amine reactive groups that are stabilized by NHS addition. The succinimide group, the end product of EDC/NHS coupling, reacts with amine groups of biological molecules such as proteins. Followed by the coupling reaction, 100 μL of protein G (0.1 mg/mL in PBS) was applied to the microfluidic chips and incubated for an hour at room temperature. To detect hemoglobin on the sensor surface, anti-hemoglobin antibody (100 μL in PBS) was immobilized by incubating for an hour at room temperature. Between surface chemistry steps, the sensor was washed with 300 μL of PBS to remove any impurities/unbound molecules.

4.6. Sample preparation

Hemoglobin and HSA solutions were prepared in 1xPBS. Hemoglobin concentrations were adjusted to 5–250 μg/mL. In specificity experiments, we applied 100 μg/mL of HSA solution to the surfaces coated with anti-hemoglobin antibodies. Sample size of each experiment was indicated on the figure captions. In plasma experiments, hemoglobin concentration was adjusted to 250 μg/mL, and applied to the surface decorated with anti-hemoglobin antibodies.

4.7. Hand-held plasmonic platform

The system utilizes a 705 nm of LED for illuminating the surface, and the incident wave is p-polarized in our configuration. A CMOS sensor is integrated to measure the amount of reflection from the surface. The platform is connected to the computer via a TV card, and we monitor the platform response on our software, which provides real-time changes in R.A. and reflection using a simple configuration of user-interface (Figs. S1–S2, Supporting Information). The hand-held biosensing system weights 1.4 lbs (0.635 kg) with a dimension of 13.5 cm × 10 cm × 5.2 cm.

4.8. Plasmonic simulations

Our calculation is based on a MATLAB program implementing transfer matrix formalism (Supplementary Information). We utilized the program to calculate reflection from our plasmonic surface by providing proper refractive index and thickness of each layer of the structure. For determining the parameters of the layers, we set the thickness of each layer to its physical dimension and then estimated the refractive index by fitting analytical results to the measured reflection spectra from the sensor.

4.9. Fourier transform infrared-attenuated total reflectance (FTIR-ATR) spectroscopy

After surface chemistry was accomplished on the sensor surface, the PMMA and DSA layers were removed for the measurements. The bare and modified gold sensors (after hemoglobin is captured) were then placed on the FTIR-ATR instrument (Thermo Fisher Scientific, Nicolet iS10, Waltham, MA, USA) and total light reflection was collected between 650 cm^{-1} and 4000 cm^{-1} range with 2 cm^{-1} of resolution.

4.10. Contact angle measurements

KRÜSS Drop Shape Analyzer (DSA100, Hamburg, Germany) instrument was used to evaluate hydrophilic behaviour of the gold sensors after the surface modification. The contact angle values were collected with sessile drop method by dropping ~5 μL of ultrapure water and calculated as the average of the contact angle values from three different drops.

4.11. Atomic force microscope (AFM) measurements

AFM was utilized as a surface-based characterization method to understand the morphology of the surface after hemoglobin binding. In the AFM measurements (Nanomagnetics Instruments, Oxford, UK), we used tapping mode. Both bare and modified gold surfaces (hemoglobin captured sensor) were attached to the AFM sample holder using double-sided carbon strip. Experimental parameters were adjusted as oscillation frequency (341.30 Hz), vibration amplitude (1 VRMS) and free vibration amplitude (2 VRMS). Imaging studies were performed with a 2 μm/s scanning rate and 256 × 256 pixels resolution. During this characterization, the raw image produced by the AFM provided an array of values of Vz (Vx, Vy), where the V represents voltages applied to the piezo drives responsible for motion in the x, y and z directions [70].

4.12. Equilibrium isotherm models

Scatchard, Langmuir, and Freundlich isotherm models provide information on host-guest binding interactions, homogenous, and heterogeneous binding of molecules to a surface, respectively [74–78].

4.13. Statistical analysis

We performed student's *t*-test using GraphPad Prism (La Jolla, CA). The statistical significance threshold was set at 0.05 ($p < 0.05$).

Declaration of Competing Interest

Prof. Utkan Demirci (UD) is a founder of and has an equity interest in: (i) DxNow Inc., a company that is developing microfluidic IVF tools and imaging technologies for point-of-care diagnostic solutions, (ii) Koek Biotech, a company that is developing microfluidic technologies for clinical solutions, (iii) Levitas Inc., a company focusing on developing microfluidic products for sorting rare cells from liquid biopsy in cancer and other diseases, and (iv) Hillel Inc., a company bringing microfluidic cell phone tools to home settings. UD's interests were viewed and managed in accordance with the conflict of interest policies.

Contributions

F.I., Y.S., and U.D. conceived the overall study and did the experimental design. F.I. and U.D. supervised the study. F.I., Y.S., and U.D.

Please cite this article as: F. Inci, Y. Saylan, A.M. Kojouri et al., A disposable microfluidic-integrated hand-held plasmonic platform for protein detection, Appl. Mater. Today, https://doi.org/10.1016/j.apmt.2019.100478

performed experiments. A.M.K. performed plasmonic simulation. F.I., Y.S., A.M.K., M.G.O., A.D., and U.D. wrote the manuscript. All authors reviewed and edited the manuscript.

Data availability

The raw data required to reproduce these findings are available from the corresponding author on reasonable request.

Acknowledgements

This work was supported by the National Institutes of Health (R01DE024971 and U54EB15408). We would like to thank Hacettepe University Scientific Research Projects Coordination Unit (No. FBI-2015-6654) for supporting Y.S. during her visit at the BAMM Labs.

Appendix A. Supplementary data

Supplementary material related to this article can be found, in the online version, at doi:https://doi.org/10.1016/j.apmt.2019.100478.

References

[1] A.P.F. Turner, Biosensors: sense and sensibility, Chem. Soc. Rev. 42 (8) (2013) 3184.
[2] M.A. Lifson, M.O. Ozen, F. Inci, S.Q. Wang, H. Inan, M. Baday, T.J. Henrich, U. Demirci, Advances in biosensing strategies for HIV-1 detection, diagnosis, and therapeutic monitoring, Adv. Drug Deliv. Rev. (2016), http://dx.doi.org/10.1016/j.addr.2016.05.018.
[3] H. Shafiee, S. Wang, F. Inci, M. Toy, T.J. Henrich, D.R. Kuritzkes, U. Demirci, Emerging technologies for point-of-care management of HIV infection, Ann. Rev. Med. (2015), http://dx.doi.org/10.1146/annurev-med-092112-143017.
[4] M. Sher, R. Zhuang, U. Demirci, W. Asghar, Paper-based analytical devices for clinical diagnosis: recent advances in the fabrication techniques and sensing mechanisms, Expert Rev. Mol. Diagn. (2017), http://dx.doi.org/10.1080/14737159.2017.1285228.
[5] S. Wang, M.A. Lifson, F. Inci, L.G. Liang, Y.F. Sheng, U. Demirci, Advances in addressing technical challenges of point-of-care diagnostics in resource-limited settings, Expert Rev. Mol. Diagn. (2016), http://dx.doi.org/10.1586/14737159.2016.1142877.
[6] S.R. Steinhubl, E.D. Muse, E.J. Topol, The emerging field of mobile health, Sci. Transl. Med. 7 (2015), 283rv3-283rv3.
[7] M. Chonchol, C. Nielson, Hemoglobin levels and coronary artery disease, Am. Heart J. 155 (2008) 494–498.
[8] A.N. Schechter, Hemoglobin research and the origins of molecular medicine, Blood 112 (2008) 3927–3938.
[9] C. Wongsrichanalai, M.J. Barcus, S. Muth, A. Sutamihardja, W.H. Wernsdorfer, A review of malaria diagnostic tools: microscopy and rapid diagnostic test (RDT), Am. J. Trop. Med. Hyg. (2007).
[10] V.A. Briand, V. Thilakarathne, R.M. Kasi, C.V. Kumar, Novel surface plasmon resonance sensor for the detection of heme at biological levels via highly selective recognition by apo-hemoglobin, Talanta 99 (2012) 113–118.
[11] S. Immenschuh, V. Vijayan, S. Janciauskiene, F. Gueler, Heme as a target for therapeutic interventions, Front. Pharmacol. 8 (2017) 146.
[12] D. Chiabrando, F. Vinchi, V. Fiorito, S. Mercurio, E. Tolosano, Heme in pathophysiology: a matter of scavenging, metabolism and trafficking across cell membranes, Front. Pharmacol. 5 (2014) 61.
[13] G. Russo, L. De Franceschi, R. Colombatti, P. Rigano, S. Perrotta, V. Voi, G. Palazzi, C. Fidone, A. Quota, G. Graziadei, A. Pietrangelo, V. Pinto, G.B. Ruffo, F. Sorrentino, D. Venturelli, M. Casale, F. Ferrara, L. Sainati, M.D. Cappellini, et al., Current challenges in the management of patients with sickle cell disease - a report of the Italian experience, Orphanet J. Rare Dis. (2019), http://dx.doi.org/10.1186/s13023-019-1099-0.
[14] J. Balla, G.M. Vercellotti, V. Jeney, A. Yachie, Z. Varga, J.W. Eaton, G. Balla, Heme, heme oxygenase and ferritin in vascular endothelial cell injury, Mol. Nutr. Food Res. (2005), http://dx.doi.org/10.1002/mnfr.200500076.
[15] I. Pal Bhowmick, N. Kumar, S. Sharma, I. Coppens, G.K. Jarori, Plasmodium falciparum enolase: stage-specific expression and sub-cellular localization, Malar. J. (2009), http://dx.doi.org/10.1186/1475-2875-8-179.
[16] S. Kumar, U. Bandyopadhyay, Free heme toxicity and its detoxification systems in human, Toxicol. Lett. (2005), http://dx.doi.org/10.1016/j.toxlet.2005.03.004.
[17] C.D. Reiter, X. Wang, J.E. Tanus-Santos, N. Hogg, R.O. Cannon, A.N. Schechter, M.T. Gladwin, Cell-free hemoglobin limits nitric oxide bioavailability in sickle-cell disease, Nat. Med. (2002), http://dx.doi.org/10.1038/nm1202-799.
[18] R. Chaudhary, A. Dubey, A. Sonker, Techniques used for the screening of hemoglobin levels in blood donors: current insights and future directions, J. Blood Med. 8 (2017) 75–88.
[19] M. Muñoz, A. Romero, J.F. Gómez, A. Manteca, E. Naveira, G. Ramírez, Utility of point-of-care haemoglobin measurement in the HemoCue-B haemoglobin for the initial diagnosis of anaemia, Clin. Lab. Haematol. (2005), http://dx.doi.org/10.1111/j.1365-2257.2005.00678.x.
[20] H. Marn, J.A. Critchley, Accuracy of the WHO haemoglobin colour scale for the diagnosis of anaemia in primary health care settings in low-income countries: a systematic review and meta-analysis, Lancet Glob. Heal. (2016), http://dx.doi.org/10.1016/S2214-109X(16)00005-X.
[21] J. Critchley, I. Bates, Haemoglobin colour scale for anaemia diagnosis where there is no laboratory: a systematic review, Int. J. Epidemiol. (2005), http://dx.doi.org/10.1093/ije/dyi195.
[22] R.G. Neville, Evaluation of portable haemoglobinometer in general practice, Br. Med. J. (Clin. Res. Ed). (1987), http://dx.doi.org/10.1136/bmj.294.6582.1263.
[23] A.M. Conway, R.F. Hinchliffe, J. Earland, L.M. Anderson, Measurement of haemoglobin using single drops of skin puncture blood: is precision acceptable? J. Clin. Pathol. (1998), http://dx.doi.org/10.1136/jcp.51.3.248.
[24] F. Inci, O. Tokel, S. Wang, U.A. Gurkan, S. Tasoglu, D.R. Kuritzkes, U. Demirci, Nanoplasmonic quantitative detection of intact viruses from unprocessed whole blood, ACS Nano 7 (2013) 4733–4745.
[25] F. Inci, C. Filippini, M. Baday, M.O. Ozen, S. Calamak, N.G. Durmus, S. Wang, E. Hanhauser, K.S. Hobbs, F. Juillard, P.P. Kuang, M.L. Vetter, M. Carocci, H.S. Yamamoto, Y. Takagi, U.H. Yildiz, D. Akin, D.R. Wesemann, A. Singhal, et al., Multitarget, quantitative nanoplasmonic electrical field-enhanced resonating device (NE^2RD) for diagnostics, Proc. Natl. Acad. Sci. U. S. A. 112 (2015) E4354–E4363.
[26] O. Tokel, F. Inci, U. Demirci, Advances in plasmonic technologies for point of care applications, Chem. Rev. 114 (2014) 5728–5752.
[27] O. Tokel, U.H. Yildiz, F. Inci, N.G. Durmus, O.O. Ekiz, B. Turker, C. Cetin, S. Rao, K. Sridhar, N. Natarajan, H. Shafiee, A. Dana, U. Demirci, Portable microfluidic integrated plasmonic platform for pathogen detection, Sci. Rep. 5 (2015).
[28] S.K. Vashist, E.M. Schneider, J.H.T. Luong, Surface plasmon resonance-based immunoassay for human C-reactive protein, Analyst (2015), http://dx.doi.org/10.1039/c5an00690b.
[29] T. Riedel, C. Rodriguez-Emmenegger, A. de los Santos Pereira, A. Bědajánková, P. Jinoch, P.M. Boltovets, E. Brynda, Diagnosis of Epstein-Barr virus infection in clinical serum samples by an SPR biosensor assay, Biosens. Bioelectron. (2014), http://dx.doi.org/10.1016/j.bios.2013.12.011.
[30] A.M.C. Lokate, J.B. Beusink, G.A.J. Besselink, G.J.M. Pruijn, R.B.M. Schasfoort, Biomolecular interaction monitoring of autoantibodies by scanning surface plasmon resonance microarray imaging, J. Am. Chem. Soc. (2007), http://dx.doi.org/10.1021/ja075103x.
[31] G.K. Joshi, S. Deitz-Mcelyea, M. Johnson, S. Mali, M. Korc, R. Sardar, Highly specific plasmonic biosensors for ultrasensitive MicroRNA detection in plasma from pancreatic cancer patients, Nano Lett. (2014), http://dx.doi.org/10.1021/nl503220s.
[32] P.K. Drain, E.P. Hyle, F. Noubary, K.A. Freedberg, D. Wilson, W.R. Bishai, W. Rodriguez, I.V. Bassett, Diagnostic point-of-care tests in resource-limited settings, Lancet Infect. Dis. (2014), http://dx.doi.org/10.1016/S1473-3099(13)70250-0.
[33] G.M. Whitesides, The origins and the future of microfluidics, Nature (2006), http://dx.doi.org/10.1038/nature05058.
[34] U.H. Yildiz, F. Inci, S. Wang, M. Toy, H.C. Tekin, A. Javaid, D.T.-Y. Lau, U. Demirci, Recent advances in micro/nanotechnologies for global control of hepatitis B infection, Biotechnol. Adv. 33 (2015) 178–190.
[35] S. Tasoglu, H. Cumhur Tekin, F. Inci, S. Knowlton, S.Q. Wang, F. Wang-Johanning, G. Johanning, D. Colevas, U. Demirci, Advances in nanotechnology and microfluidics for human papillomavirus diagnostics, Proc. IEEE 103 (2015) 161–178.
[36] R. Zia, J.A. Schuller, A. Chandran, M.L. Brongersma, Plasmonics: the next chip-scale technology, Mater. Today 9 (2006) 20–27.
[37] A. Olaru, C. Bala, N. Jaffrezic-Renault, H.Y. Aboul-Enein, Surface plasmon resonance (SPR) biosensors in pharmaceutical analysis, Crit. Rev. Anal. Chem. 45 (2015) 97–105.
[38] A.P.F. Turner, Biosensors—sense and sensitivity, Science (80-.) 290 (2000) 1315–1317.
[39] H. Wei, S.M. Hossein Abtahi, P.J. Vikesland, Plasmonic colorimetric and SERS sensors for environmental analysis, Environ. Sci. Nano (2015), http://dx.doi.org/10.1039/c4en00211c.
[40] F. Yesilkoy, R.A. Terborg, J. Pello, A.A. Belushkin, Y. Jahani, V. Pruneri, H. Altug, Phase-sensitive plasmonic biosensor using a portable and large field-of-view interferometric microarray imager, Light Sci. Appl. (2018), http://dx.doi.org/10.1038/lsa.2017.152.
[41] A.E. Cetin, A.F. Coskun, B.C. Galarreta, M. Huang, D. Herman, A. Ozcan, H. Altug, Handheld high-throughput plasmonic biosensor using computational on-chip imaging, Light Sci. Appl. (2014), http://dx.doi.org/10.1038/lsa.2014.3.
[42] Y. Liu, Q. Liu, S. Chen, F. Cheng, H. Wang, W. Peng, Surface plasmon resonance biosensor based on smart phone platforms, Sci. Rep. (2015), http://dx.doi.org/10.1038/srep12864.
[43] M. Trzaskowski, A. Napiórkowska, E. Augustynowicz-Kopeć, T. Ciach, Detection of tuberculosis in patients with the use of portable SPR device,

Sens. Actuators B Chem. (2018), http://dx.doi.org/10.1016/j.snb.2017.12.183.
[44] S. Wang, J. Xie, M. Jiang, K. Chang, R. Chen, L. Ma, J. Zhu, Q. Guo, H. Sun, J. Hu, The development of a portable SPR bioanalyzer for sensitive detection of Escherichia coli O157:H7, Sensors (Switzerland) (2016), http://dx.doi.org/10.3390/s16111856.
[45] F. Fernández, K. Hegnerová, M. Piliarik, F. Sanchez-Baeza, J. Homola, M.P. Marco, A label-free and portable multichannel surface plasmon resonance immunosensor for on site analysis of antibiotics in milk samples, Biosens. Bioelectron. (2010), http://dx.doi.org/10.1016/j.bios.2010.06.012.
[46] X.L. Zhang, Y. Liu, T. Fan, N. Hu, Z. Yang, X. Chen, Z.Y. Wang, J. Yang, Design and performance of a portable and multichannel SPR device, Sensors (Switzerland) (2017), http://dx.doi.org/10.3390/s17061435.
[47] R. Kurita, Y. Yokota, Y. Sato, F. Mizutani, O. Niwa, On-chip enzyme immunoassay of a cardiac marker using a microfluidic device combined with a portable surface plasmon resonance system, Anal. Chem. (2006), http://dx.doi.org/10.1021/ac060480y.
[48] H. Šípová, M. Piliarik, M. Vala, K. Chadt, P. Adam, M. Bocková, K. Hegnerová, J. Homola, Portable surface plasmon resonance biosensor for detection of nucleic acids, Procedia Eng. (2011), http://dx.doi.org/10.1016/j.proeng.2011.12.037.
[49] P. Preechaburana, M.C. Gonzalez, A. Suska, D. Filippini, Surface plasmon resonance chemical sensing on cell phones, Angew. Chem. (2012), http://dx.doi.org/10.1002/ange.201206804.
[50] J. Homola, Surface plasmon resonance sensors for detection of chemical and biological species, Chem. Rev. (2008), http://dx.doi.org/10.1021/cr068107d.
[51] A. Abbas, M.J. Linman, Q. Cheng, New trends in instrumental design for surface plasmon resonance-based biosensors, Biosens. Bioelectron. (2011), http://dx.doi.org/10.1016/j.bios.2010.09.030.
[52] J.N. Anker, W.P. Hall, O. Lyandres, N.C. Shah, J. Zhao, R.P. Van Duyne, Biosensing with plasmonic nanosensors, Nat. Mater. (2008), http://dx.doi.org/10.1038/nmat2162.
[53] J.L. Hammond, N. Bhalla, S.D. Rafiee, P. Estrela, Localized surface plasmon resonance as a biosensing platform for developing countries, Biosensors (2014), http://dx.doi.org/10.3390/bios4020172.
[54] J.M. Rooney, E.A.H. Hall, Surface plasmon resonance: theoretical evolutionary design optimization for a model analyte sensitive absorbing-layer system, Anal. Chem. (2005), http://dx.doi.org/10.1021/ac0496751.
[55] M. Piliarik, M. Vala, I. Tichý, J. Homola, Compact and low-cost biosensor based on novel approach to spectroscopy of surface plasmons, Biosens. Bioelectron. (2009), http://dx.doi.org/10.1016/j.bios.2008.11.003.
[56] A.N. Naimushin, S.D. Soelberg, D.U. Bartholomew, J.L. Elkind, C.E. Furlong, A portable surface plasmon resonance (SPR) sensor system with temperature regulation, Sens. Actuators B Chem. (2003), http://dx.doi.org/10.1016/S0925-4005(03)00533-1.
[57] S. Scarano, M. Mascini, A.P.F. Turner, M. Minunni, Surface plasmon resonance imaging for affinity-based biosensors, Biosens. Bioelectron. 25 (2010) 957–966.
[58] Y. Lee, D. Jang, K.-S. Lee, W. Kim, Y.-S. Sohn, Enhancing performance of a miniaturized surface plasmon resonance sensor in the reflectance detection mode using a waveguide-coupled bimetallic chip, Nanoscale Res. Lett. (2013), http://dx.doi.org/10.1186/1556-276X-8-344.
[59] N.S. Ghatpande, P.P. Apte, B.N. Joshi, S.S. Naik, D. Bodas, V. Sande, P. Uttarwar, P.P. Kulkarni, Development of a novel smartphone-based application for accurate and sensitive on-field hemoglobin measurement, RSC Adv. (2016), http://dx.doi.org/10.1039/c6ra24366e.
[60] R.G. Mannino, D.R. Myers, E.A. Tyburski, C. Caruso, J. Boudreaux, T. Leong, G.D. Clifford, W.A. Lam, Smartphone app for non-invasive detection of anemia using only patient-sourced photos, Nat. Commun. 9 (2018), 4924.
[61] D. Mabey, R.W. Peeling, A. Ustianowski, M.D. Perkins, Diagnostics for the developing world, Nat. Rev. Microbiol. (2004), http://dx.doi.org/10.1038/nrmicro841.
[62] G. Wu, M.H. Zaman, Low-cost tools for diagnosing and monitoring HIV infection in low-resource settings, Bull. World Health Organ. (2012), http://dx.doi.org/10.2471/BLT.12.102780.
[63] W.G. Lee, Y.G. Kim, B.G. Chung, U. Demirci, A. Khademhosseini, Nano/Microfluidics for diagnosis of infectious diseases in developing countries, Adv. Drug Deliv. Rev. (2010), http://dx.doi.org/10.1016/j.addr.2009.11.016.
[64] E. Palik, Handbook of Optical Constants of Solids. Handb. Opt. Constants Solids, 1997, http://dx.doi.org/10.1016/B978-012544415-6.50143-6, 1059.
[65] J. Vörös, The density and refractive index of adsorbing protein layers, Biophys. J. 87 (2004) 553–561.
[66] J.A. De Feijter, J. Benjamins, F.A. Veer, Ellipsometry as a tool to study the adsorption behavior of synthetic and biopolymers at the air–water interface, Biopolymers 17 (1978) 1759–1772.
[67] J. Piehler, A. Brecht, G. Gauglitz, Affinity detection of low molecular weight analytes, Anal. Chem. 68 (1996) 139–143.
[68] K.L. Prime, G.M. Whitesides, Self-assembled organic monolayers: model systems for studying adsorption of proteins at surfaces, Science (80-.) 252 (1991) 1164–1167.
[69] J. Canning, J. Qian, K. Cook, Large dynamic range SPR measurements using a ZnSe prism, Photonic Sens. (2015), http://dx.doi.org/10.1007/s13320-015-0262-z.
[70] A.A.G. Requicha, S. Meltzer, F.P.T. Arce, J.H. Makaliwe, H. Sikén, S. Hsieh, D. Lewis, B.E. Koel, M.E. Thompson, Manipulation of nanoscale components with the AFM: principles and applications, Proc. IEEE Conf. Nanotechnol. (2001) 81–86, http://dx.doi.org/10.1109/NANO.2001.966398.
[71] G. Durmus, E.N. Taylor, K.M. Kummer, F. Inci, K.M. Tarquinio, T.J. Webster, Fructose-enhanced reduction of bacterial growth on nanorough surfaces, Int. J. Nanomed. 7 (2012) 537.
[72] F. Inci, U. Celik, B. Turken, H.Ö. Özer, F.N. Kok, Construction of P-glycoprotein incorporated tethered lipid bilayer membranes, Biochem. Biophys. Rep. 2 (2015) 115–122.
[73] X. Li, S.M. Husson, Adsorption of dansylated amino acids on molecularly imprinted surfaces: a surface plasmon resonance study, Biosens. Bioelectron. (2006), http://dx.doi.org/10.1016/j.bios.2006.04.016.
[74] M.S. Rocha, Extracting physical chemistry from mechanics: a new approach to investigate DNA interactions with drugs and proteins in single molecule experiments, Integr. Biol. (United Kingdom) 7 (2015) 967–986.
[75] H. Dibekkaya, Y. Saylan, F. Yılmaz, A. Derazshamshir, A. Denizli, Surface plasmon resonance sensors for real-time detection of cyclic citrullinated peptide antibodies, J. Macromol. Sci. Part A Pure Appl. Chem. 53 (2016).
[76] I. Langmuir, The constitution and fundamental properties of solids and liquids. Part I. Solids, J. Am. Chem. Soc. 38 (1916) 2221–2295.
[77] T. Fornstedt, P. Forssén, J. Samuelsson, Modeling of preparative liquid chromatography, Liq. Chromatogr. (2013) 407–425, http://dx.doi.org/10.1016/B978-0-12-415807-8.00018-3.
[78] Y. Saylan, F. Yılmaz, A. Derazshamshir, E. Yılmaz, A. Denizli, Synthesis of hydrophobic nanoparticles for real-time lysozyme detection using surface plasmon resonance sensor, J. Mol. Recognit. 30 (2017).
[79] L. Uzun, R. Say, S. Unal, A. Denizli, Production of surface plasmon resonance based assay kit for hepatitis diagnosis, Biosens. Bioelectron. 24 (2009) 2878–2884.
[80] A.J. Saah, D.R. Hoover, 'Sensitivity' and 'specificity' reconsidered: the meaning of these terms in analytical and diagnostic settings, Ann. Intern. Med. 126 (1997) 91–94.
[81] S. Barbosa, P. Taboada, V. Mosquera, Fibrillation and polymorphism of human serum albumin, Bionanoimaging (2014) 345–362, http://dx.doi.org/10.1016/B978-0-12-394431-3.00032-8.
[82] A.R. Statz, R.J. Meagher, A.E. Barron, P.B. Messersmith, New peptidomimetic polymers for antifouling surfaces, J. Am. Chem. Soc. (2005), http://dx.doi.org/10.1021/ja0522534.
[83] Z. Lu, Z. Chen, Y. Guo, Y. Ju, Y. Liu, R. Feng, C. Xiong, C.K. Ober, L. Dong, Flexible hydrophobic antifouling coating with oriented nanotopography and nonleaking capsaicin, ACS Appl. Mater. Interfaces (2018), http://dx.doi.org/10.1021/acsami.7b19436.
[84] A. Miodek, E.M. Regan, N. Bhalla, N.A.E. Hopkins, S.A. Goodchild, P. Estrela, Optimisation and characterisation of anti-fouling ternary SAM layers for impedance-based aptasensors, Sensors (Switzerland) (2015), http://dx.doi.org/10.3390/s151025015.
[85] T. Lakshmipriya, M. Fujimaki, S.C.B. Gopinath, K. Awazu, Y. Horiguchi, Y. Nagasaki, A high-performance waveguide-mode biosensor for detection of factor IX using PEG-based blocking agents to suppress non-specific binding and improve sensitivity, Analyst (2013), http://dx.doi.org/10.1039/c3an00298e.
[86] M.V. Riquelme, H. Zhao, V. Srinivasaraghavan, A. Pruden, P. Vikesland, M. Agah, Optimizing blocking of nonspecific bacterial attachment to impedimetric biosensors, Sens. Biosensing Res. (2016), http://dx.doi.org/10.1016/j.sbsr.2016.04.003.
[87] Y. Nagasaki, Construction of a densely poly(ethylene glycol)-chain-tethered surface and its performance, Polym. J. (2011), http://dx.doi.org/10.1038/pj.2011.93.
[88] C. Nogues, H. Leh, J. Lautru, O. Delelis, M. Buckle, Efficient antifouling surface for quantitative surface plasmon resonance based biosensor analysis, PLoS One (2012), http://dx.doi.org/10.1371/journal.pone.0044287.
[89] J.L. Arlett, E.B. Myers, M.L. Roukes, Comparative advantages of mechanical biosensors, Nat. Nanotechnol. (2011), http://dx.doi.org/10.1038/nnano.2011.44.
[90] Y. Liu, W.D. Wilson, Quantitative analysis of small molecule-nucleic acid interactions with a biosensor surface and surface plasmon resonance detection, Methods Mol. Biol. (2010).
[91] Ö. Erdem, Y. Saylan, N. Cihangir, A. Denizli, Molecularly imprinted nanoparticles based plasmonic sensors for real-time Enterococcus faecalis detection, Biosens. Bioelectron. (2019), http://dx.doi.org/10.1016/j.bios.2018.11.030.
[92] F. Inci, M.O. Ozen, Y. Saylan, M. Miansari, D. Cimen, R. Dhara, T. Chinnasamy, M. Yuksekkaya, C. Filippini, D.K. Kumar, S. Calamak, Y. Yesil, N.G. Durmus, G. Duncan, L. Klevan, U. Demirci, A novel on-chip method for differential extraction of sperm in forensic cases, Adv. Sci. (2018), http://dx.doi.org/10.1002/advs.201800121.
[93] W. Asghar, M. Yuksekkaya, H. Shafiee, M. Zhang, M.O. Ozen, F. Inci, M. Kocakulak, U. Demirci, Engineering long shelf life multi-layer biologically active surfaces on microfluidic devices for point of care applications, Sci. Rep. 6 (2016).
[94] Y. Yang, Y. Long, Z. Li, N. Li, K. Li, F. Liu, Real-time molecular recognition between protein and photosensitizer of photodynamic therapy by quartz crystal microbalance sensor, Anal. Biochem. 392 (2009) 22–27.

Please cite this article as: F. Inci, Y. Saylan, A.M. Kojouri et al., A disposable microfluidic-integrated hand-held plasmonic platform for protein detection, Appl. Mater. Today, https://doi.org/10.1016/j.apmt.2019.100478

[95] A.K. Tatikonda, M. Tkachev, R. Naaman, A highly sensitive hybrid organic-inorganic sensor for continuous monitoring of hemoglobin, Biosens. Bioelectron. 45 (2013) 201–205.
[96] Y. Wang, Y. Zhou, J. Sokolov, B. Rigas, K. Levon, M. Rafailovich, A potentiometric protein sensor built with surface molecular imprinting method, Biosens. Bioelectron. 24 (1) (2008) 162–166.
[97] Data Sheet for NBK7, 2018, https://www.sydor.com/wp-content/uploads/SCHOTT-N-BK-7-Optical-Glass.pdf. (Accessed 28 August 2018).
[98] H. Hinterwirth, S. Kappel, T. Waitz, T. Prohaska, W. Lindner, M. Lämmerhofer, Quantifying thiol ligand density of self-assembled monolayers on gold nanoparticles by inductively coupled plasma-mass spectrometry, ACS Nano 7 (2013) 1129–1136.
[99] M.L. Jeong, K.P. Hyun, Y. Jung, K.K. Jin, O.J. Sun, H.C. Bong, Direct immobilization of protein G variants with various numbers of cysteine residues on a gold surface, Anal. Chem. 79 (2007) 2680–2687.
[100] R.L. Schoch, L.E. Kapinos, R.Y.H. Lim, Nuclear transport receptor binding avidity triggers a self-healing collapse transition in FG-nucleoporin molecular brushes, Proc. Natl. Acad. Sci. U. S. A. 109 (2012) 16911–16916.

Please cite this article as: F. Inci, Y. Saylan, A.M. Kojouri et al., A disposable microfluidic-integrated hand-held plasmonic platform for protein detection, Appl. Mater. Today, https://doi.org/10.1016/j.apmt.2019.100478